209. Synthesis, Reactivity, and Fluxional Behaviour of $[Ir_2Rh_2(CO)_{12}]$, and Crystal Structure of $[Ir_2Rh_2(CO)_8(norbornadiene)_2]$

by **Giacomo Bondietti, Gianfranco Suardi, Renzo Ros**[1]) and **Raymond Roulet***

Institut de Chimie Minérale et Analytique de l'Université, 3, place du Château, CH–1005 Lausanne

and **Fabrizia Grepioni** and **Dario Braga**

Dipartimento di Chimica 'G. Ciamician', Università di Bologna, Via Selmi 2, I–40126 Bologna

(21.VI.93)

The synthesis of $[Ir_2Rh_2(CO)_{12}]$ (**1**) by the literature method gives a mixture **1**/$[IrRh_3(CO)_{12}]$ which cannot be separated using chromatography. The reaction of $[Ir(CO)_4]^-$ with 1 mol-equiv. of $[Rh(CO)_2(THF)_2]^+$ in THF gives pure **1** in 61% yield. Crystals of **1** are highly disordered, unlike those of its derivative $[Ir_2Rh_2(CO)_5(\mu_2\text{-}CO)_3(norbornadiene)_2]$ which were analysed using X-ray diffraction. The ground-state geometry of **1** in solution has three edge-bridging CO's on the basal $IrRh_2$ face of the metal tetrahedron. Time averaging of CO's takes place above 230 K. The CO site exchange of lowest activation energy is due to one synchronous change of basal face, as shown by 2D- and VT- ^{13}C-NMR. Substitution of CO by X^- in **1** takes place at a Rh-atom giving $[Ir_2Rh_2(CO)_8(\mu_2\text{-}CO)_3X]^-$ (X = Br, I). Substitution by bidentate ligands gives $[Ir_2Rh_2(CO)_7(\mu_2\text{-}CO)_3(\eta^4\text{-}L)]$ (L = norbornadiene, cycloocta-1,5-diene) where the ligand L is chelating a Rh-atom of the basal $IrRh_2$ face. Carbonyl substitution by tridentate ligands gives $[Ir_2Rh_2(CO)_6(\mu_2\text{-}CO)_3(\mu_3\text{-}L)]$ (L = 1,3,5-trithiane, tripod) with L capping the triangular basal face of the metal tetrahedron. Carbonyl scrambling is also observed in these substituted derivatives of **1** and is mainly due to the rotation of three terminal CO's about a local C_3 axis on the apical Ir-atom.

Introduction. – The tetrahedral carbonyl cluster compounds of mixed d^9 metals known to date are $[Co_xRh_{4-x}(CO)_{12}]$, $[Co_xIr_{4-x}(CO)_{12}]$, and $[Ir_xRh_{4-x}(CO)_{12}]$ ($x = 2, 3$) [1]. $[Co_2Ir_2(CO)_{12}]$ has been structurally characterised by X-ray analysis [2], and the geometry of $[Co_3Rh(CO)_{12}]$ in solution has been established by ^{13}C-NMR spectroscopy [3]. $[CoRh_3(CO)_{12}]$ and $[CoIr_3(CO)_{12}]$ are thermally unstable [1] [4]. In contrast, the unreported $[Ir_3Rh(CO)_{12}]$ is quite stable, and its synthesis as well as that of 16 of its derivatives have now been achieved [5].

In our hands, the reported synthesis of $[Ir_2Rh_2(CO)_{12}]$ (**1**) gave repeatedly a mixture **1**/$[IrRh_3(CO)_{12}]$ (10–15%). The observation of peaks corresponding to $[IrRh_3(CO)_n]^+$ ions (*ca.* 10%) in the original mass spectrum of **1** was attributed to redistribution phenomena in the gas phase, but could also be explained by an impurity of $[IrRh_3(CO)_{12}]$. The presence of $[IrRh_3(CO)_{12}]$ in the mixture cannot be detected by IR spectroscopy due to band overlaps, but was identified in a ^{13}C-NMR spectrum of sample of the product enriched in ^{13}CO. Unfortunately, these two mixed cluster compounds are exceedingly difficult to separate using TLC, HPLC, *Lobar*, or conventional elution chromatography, and by fractional crystallisation or sublimation. The reasons for the formation of $[IrRh_3(CO)_{12}]$ during the original synthesis of **1** have now been identified, and we report

[1]) Permanent address: Istituto di Chimica dell'Università, Via Marzolo 9, I–35131 Padova.

here on a modified synthesis giving pure **1** in 61% yields, on its fluxional behaviour in solution as studied with 2D-^{13}C-NMR spectroscopy, on the synthesis of some substituted derivatives, and on the crystal structure of $[Ir_2Rh_2(CO)_8(norbornadiene)_2]$.

Synthesis and Fluxional Behaviour of $[Ir_2Rh_2(CO)_{12}]$. – The original synthesis of **1** was attained by the redox condensation of $[Ir(CO)_4]^-$, prepared *in situ* from $[Ir_4(CO)_{12}]$, with the dimer $[Rh(CO)_2Cl]_2$. It is now known that on reacting $[Ir_4(CO)_{12}]$ with excess Na in THF, the formed $Na[Ir(CO)_4]$ may be further reduced to $Na_3[Ir(CO)_3]$ [6]. We have found that the latter reacts with 3 mol-equiv. of Rh^I to form $[IrRh_3(CO)_{12}]$ in 90% yields. Therefore, $[Ir(CO)_4]^-$ should be isolated, *e.g.* as the PPN^+ salt [7], prior to the redox condensation. We have also found that rapid substitution of one CO ligand of **1** by Cl^- takes place in THF giving $[Ir_2Rh_2(CO)_{11}Cl]^-$ which is thermally unstable and decomposes, above −50°, to $[Rh(CO)_2Cl_2]^-$ and other unidentified products. Therefore, the presence of Cl^- should be avoided, *e.g.* by prior bridge-splitting of the Rh-dimer with $AgPF_6$ in THF giving $[Rh(CO)_2(THF)_2]^+$ [8]. The modified redox condensation (*Eqn. 1*) gives pure **1** in 61% yields after recrystallisation (no chromatography is needed).

$$2\,PPN[Ir(CO)_4] + 2[Rh(CO)_2(THF)_2]PF_6 \xrightarrow{THF,\,-50°} [Ir_2Rh_2(CO)_{12}] + 2\,[PPN]PF_6 \quad (1)$$

The orange crystals of **1** were found highly disordered and unfit for X-ray analysis. A solid-state ^{13}C-NMR spectrum of a sample enriched in ^{13}CO (*ca.* 30%) at 298 K exhibits seven signals at 224.7, 211.3, 179.8, 167.3, 164.6, 158.6, and 152.3 ppm; the resonances above 200 ppm indicate the presence of edge-bridging CO ligands. The slow-exchange limiting ^{13}C-NMR spectrum of the same sample in CD_2Cl_2 was observed at 220 K and contained eight resonances with relatives intensities 1:2:2:1:2:2:1:1 at 223.3 (*td*, J(C,Rh) = 29, J(C,C) = 8, *a*); 211.3 (*dd*, J(C,Rh) = 27, J(C,C) = 8, *b*); 180.0 (*d*, ^1J(C,Rh) = 76, *d*); 167.9 (*s*, *f*); 165.8 (*s*, *g*); 164.8 (*d*, ^1J(C,Rh) = 61, *c*); 158.7 (*s*); 153.7 (*s*) (*e* and *h*). Their assignment (*Scheme 1*, left) was based on the C,Rh couplings and on the general observation that, in the ^{13}C- and ^{31}P-NMR spectra of Ir_4 cluster compounds, the δ's of the ligand resonances decrease in the positional sequence bridging > radial > axial ≈ apical [9]. The two resonances at highest δ's appear in the region characteristic of bridging CO's, and their multiplicity and relative intensities indicate that the two Rh-atoms are located on the basal face of the metal tetrahedron. It is known that in carbonyltetrairidium clusters, the CO's with greatest C,C coupling constants are in

Scheme 1

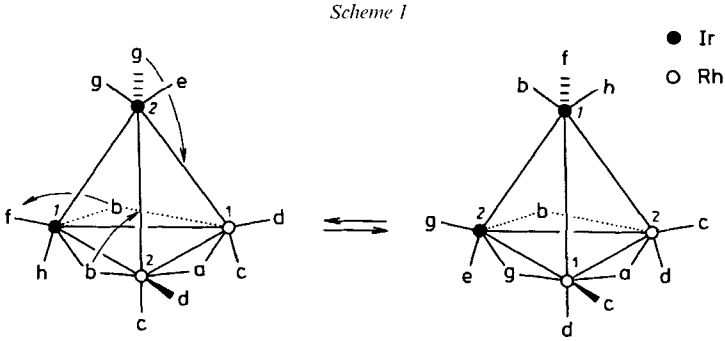

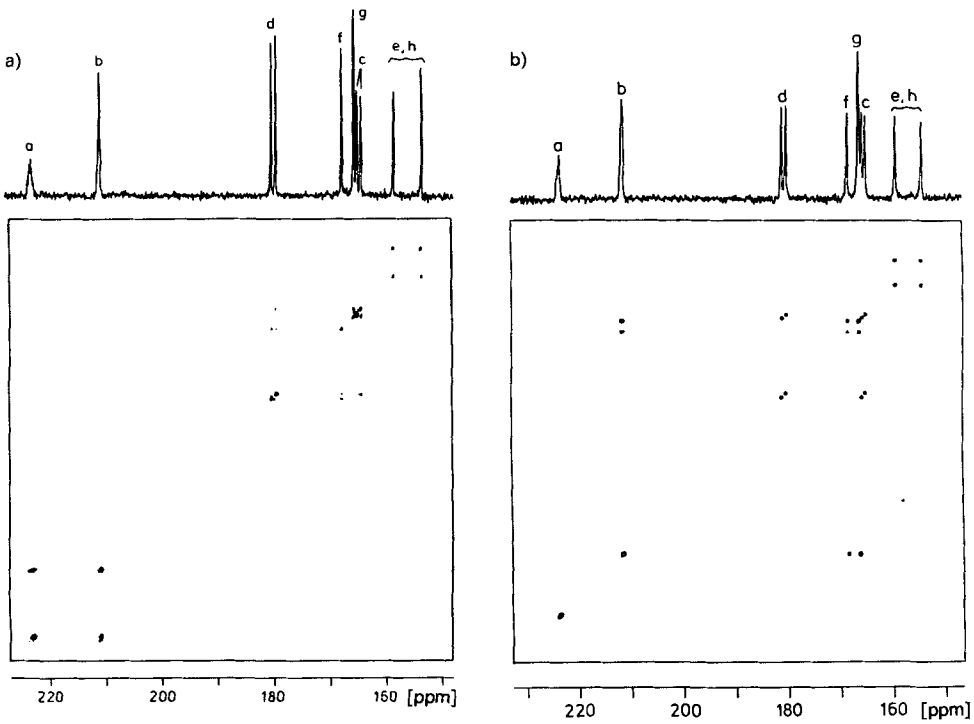

Fig. 1. a) *2D-COSY ^{13}C-NMR Spectrum of* **1** *in CD_2Cl_2 at 235 K* (F2 = 7142.8, F1 = 3571.4 Hz); b) *EXSY spectrum of* **1** *in CD_2Cl_2 at 243 K* (mixing time: 100 ms, F2 = 7812.4, F1 = 3096.2 Hz)

relative pseudo-*trans*-positions (in particular, geminal ^2J(CO,CO) are very small) [10]. A 2D-COSY spectrum in CD_2Cl_2 at 235 K (*Fig. 1, a*) shows couplings (12 ± 1 Hz) between the signals at 165.8 (*c*) and 164.8 ppm (*g*), and 158.7 and 153.7 ppm (*e* and *h*). The corresponding pairs of CO's are thus in relative pseudo-*trans*-positions. The assignment of CO's *e* and *h* remains ambiguous, but fortunately will be of no importance in the discussion of the fluxionality of **1**. A weaker C,C coupling is observed between the signals at 180.0 (*d*) and 167.9 ppm (*f*) which corresponds to CO's in pseudo-*cis*-positions, and *d* is distinguished from *f* by its C,Rh coupling. The C_s geometry of **1** in solution is similar to that found for $[Co_2Rh_2(CO)_{12}]$ in the solid state [2], with Ir-atoms replacing the two Co-atoms.

An EXSY ^{13}C-NMR spectrum of **1** at 243 K (*Fig. 1, b*) shows the dynamic connectivities $b \leftrightarrow f \leftrightarrow g$, $d \leftrightarrow c$, and $e \leftrightarrow h$. Carbonyl *a* remains unaffected, excluding site exchanges by a merry-go-round of six basal CO's, as postulated for $[Rh_4(CO)_{12}]$ [11]. Since axial-basal CO site exchanges are observed, the fluxional process of lowest activation energy is clearly the change of basal face by synchronous edge-bridging of three CO's on the triangular face (Rh(1)–Rh(2)–Ir(2)) (*Scheme 1*). This face is indeed the only one which is equivalent to the original basal face (Rh(1)–Rh(2)–Ir(1)) through rotation around the C_2 axis of the metal framework. The process must be synchronous, *i.e.* not passing through an unbridged intermediate, since CO *a* does not exchange with terminal CO's. CO

Bridging to any of the other two faces of the metal tetrahedron is excluded, since it would require an $a \leftrightarrow b$ exchange, which is not observed, and would lead to a structure with an apical Rh-atom which is not equivalent in energy to the ground-state structure. It is remarkable that the Rh-atoms in **1** seem to retain as many bridging CO ligands (which are better π acceptors than those in terminal positions) as possible during the intramolecular site exchanges. The same behaviour has been recently observed for $[IrRh_3(CO)_{12}]$ [12], in contrast with the facile μ_2-CO$\leftrightarrow\eta$-CO exchanges observed for $[Ir_4(CO)_9$(1,3,5-trithiane)] [13] ($[Ir_4(CO)_{12}]$ and $[Ir_3Rh(CO)_{12}]$ are too insoluble in common organic solvents to be studied using NMR).

Line-shape analysis [14] of the variable-temperature ^{13}C-NMR spectra was carried out using the following *Kubo-Sack* matrix elements: $(d, d) = (f, f) = (c, c) = (e, e) = (h, h) = -k$, $(d, c) = (c, d) = (h, e) = (e, h) = k$, $(b, b) = -k/2$, $(g, f) = (g, b) = k/2$, with k = rate constant of the CO site exchange. An example of the obtained and simulated

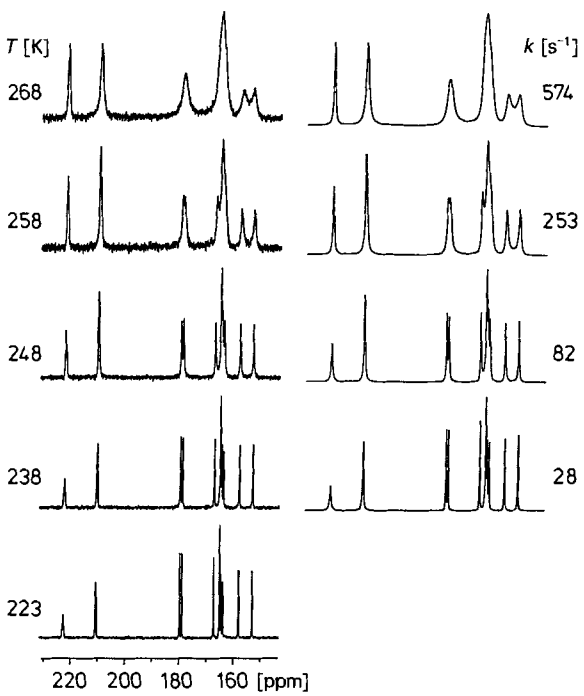

Fig. 2. *Experimental and calculated variable-temperature ^{13}C-NMR spectra of* **1** *in CD_2Cl_2*

spectra is given in *Fig. 2*. A plot of ln k *vs.* $1/T$ gave a free enthalpy of activation of 51.2 ± 0.4 kJ mol^{-1} at 298 K. Above 273 K, other site exchanges involving CO *a* start to operate, but these could not be identified as the signals were too broad to establish the dynamic connectivities from EXSY experiments.

Synthesis of Some Substituted Derivatives of $[Ir_2Rh_2(CO)_{12}]$. – The reaction of **1** with a slight excess of $[NEt_4]X$ in CH_2Cl_2 at 0° gives the red clusters $NEt_4[Ir_2Rh_2(CO)_{11}X]$

(X = Br, **2**; X = I, **3**) in good yields. They are stable in solution under N_2, but revert back to **1** under CO (1 atm). $[Ir_2Rh_2(CO)_{11}Cl]^-$ is thermally unstable, and could only be identified in solution at 220 K (see *Exper. Part*).

The IR spectra of **2** and **3** show two absorptions below 1900 cm^{-1} indicating the presence of bridging CO's. The slow-exchange limiting ^{13}C-NMR spectra of samples enriched in ^{13}CO (*ca.* 30%) in CD_2Cl_2 are observed at 220 K and are quite similar, each with a pattern of eleven resonances indicating C_1 symmetry (see *Experimental*). The presence of three signals with δ's in the region of bridging CO's and of three *doublets* with $^1J(C,Rh)$ values typical for terminal CO's indicate that the substitution of CO by X^- took place as expected on one of the Rh-atoms of the $IrRh_2$ basal face (*Scheme 2*, left). The assignment of the signals was based on a 2D-COSY spectrum of **3** in CD_2Cl_2 at 220 K (*Fig. 3, a*). The C,C couplings (12 ± 1 Hz), observed between the two *doublets* with δ's in the region of radial CO's (186 and 183 ppm), are in agreement with a geometry with two radial CO's in pseudo-*trans*-positions, each bonded to one Rh-atom. Each *doublet* couples with the *singlet* at 172 ppm which can thus be assigned to the radial CO bonded to the basal Ir-atom (*f*). The final two pseudo-*trans*-C,C couplings are related to the pairs of CO's (*c*, *g*) and (*h*, *e*) proving that the X^- ligand is located in an axial position.

An EXSY spectrum of **3** in CD_2Cl_2 at 250 K shows the dynamic connectivities $e \leftrightarrow g \leftrightarrow g'$ (*Fig. 3, b*, showing the terminal CO region). Transfer of magnetisation was not observed between the bridging and the terminal CO's. The scrambling process of lowest activation energy in **2** and **3** is, therefore, localised on the apical Ir-atom and is due to the rotation of 3 CO's about the local C_3 axis (*Scheme 2*). Simulation of the variable-temperature ^{13}C-NMR spectra with the corresponding three sites exchange matrix gave a free enthalpy of activation at 298 K of 54.6 ± 0.7 for **2**, and 58.8 ± 0.5 kJ mol^{-1} for **3**. The fluxional process of lowest activation energy in $[Ir_4(CO)_{11}X]^-$ is the merry-go-round of the six basal CO's ($\Delta G^{\neq}_{298}$ = 37 ± 1 kJ mol^{-1} for $X = Br^-$ and I^- [15]). Once again, substitution of the Ir by the Rh-atom in the metal framework slows the fluxional processes, in particular those requiring the interconversion of μ_2- and η-CO bonding modes at two Rh-centres. These processes only start to contribute significantly to axial-basal exchanges above room temperature.

The reactions of **1** with 1 mol-equiv. of norbornadiene (nbd) or cycloocta-1,5-diene (cod) in CH_2Cl_2 at room temperature gave $[Ir_2Rh_2(CO)_{10}(\eta^4\text{-nbd})]$ (**4**) and

Scheme 2

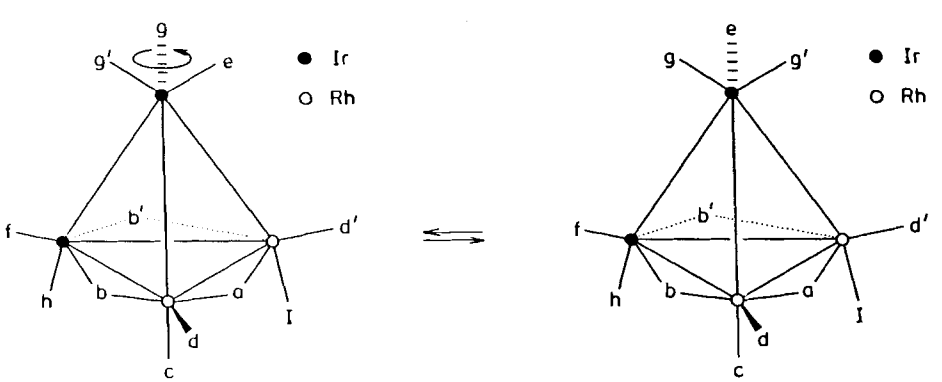

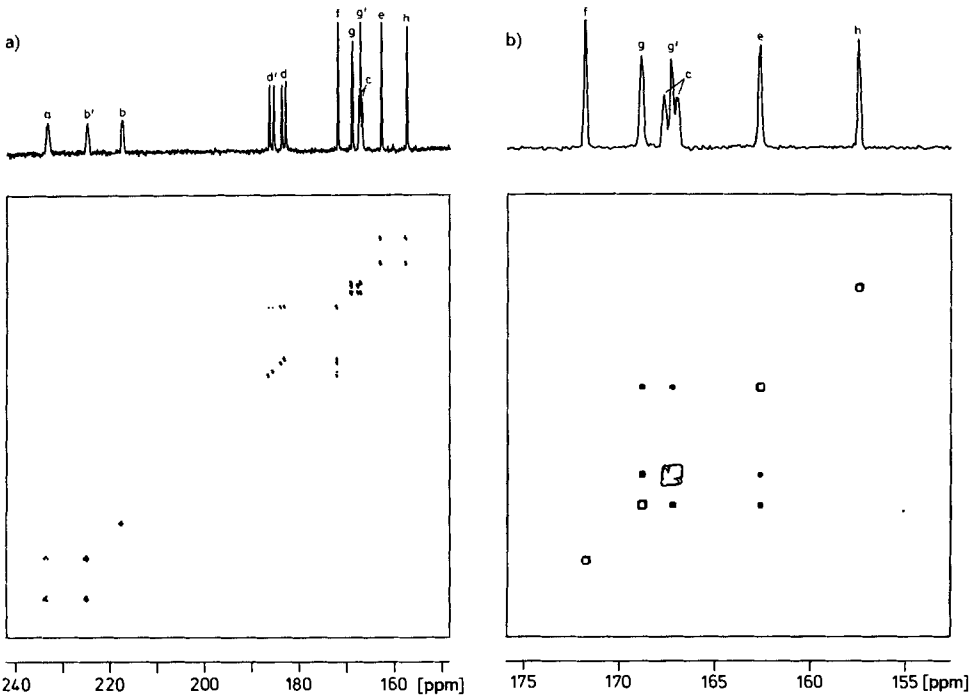

Fig. 3. a) *2D-COSY ^{13}C-NMR Spectrum of* **3** *in CD_2Cl_2 at 220 K* ($F2$ = 8474.6, $F1$ = 4237.3 Hz); b) *EXSY spectrum of* **3** *in CD_2Cl_2 at 250 K* (region of terminal CO's, mixing time: 50 ms, same $F1$ and $F2$ as in *a*)

$[Ir_2Rh_2(CO)_{10}(\eta^4\text{-cod})]$ (**5**), respectively. Clusters **4** and **5** are stable in solution under N_2, but revert back to **1** under CO (1 atm). This property can be used for the enrichment of **1** in ^{13}CO. The IR spectra of **4** and **5** show each three absorptions below 1900 cm^{-1} characteristic of bridging CO's. The slow-exchange limiting ^{13}C-NMR spectra of samples enriched in ^{13}CO (*ca.* 30%) in CD_2Cl_2 are observed at 190 K and exhibit ten resonances in the CO region indicating C_1 symmetry (see *Exper. Part*). The multiplicities, due to C,Rh couplings, of the three signals with δ's in the region of bridging CO's indicate that the basal face of the clusters contain one Ir- and two Rh-atoms. The presence of one *doublet* (^1J(C,Rh) $\approx$ 75 Hz) with δ in the region of radial CO's (*d*) and only one other *doublet* (^1J(C,Rh) $\approx$ 62 Hz) in the region of axial CO's (*c*) indicates that the diolefin chelates one basal Rh-atom (*Scheme 3*, left). The analogous cluster $[Ir_4(CO)_{10}(\eta^4\text{-cod})]$ [16] [17], whose crystal structure is known [17], has C_s symmetry. Cluster **5** having two Ir-atoms replaced by Rh would also have C_s symmetry, if the diolefin were bonded to a basal Ir-atom. As it has C_1 symmetry, the diolefin must indeed be bonded to Rh. Inspection of a 2D-COSY spectrum of **5** in the region of terminal CO's shows C,C coupling between the signals assigned to the pairs of carbonyls (*d*,*f*), (*g*,*c*), and (*e*,*h*), confirming their relative pseudo-*trans*-positions. An EXSY spectrum of **5** in CD_2Cl_2 at 268 K shows the dynamic connectivities $b \leftrightarrow g'$, $d \leftrightarrow c$, $f \leftrightarrow g$, $h \leftrightarrow e$, and $g \leftrightarrow g' \leftrightarrow e$ (*Fig. 4*, *a*). The latter corresponds to the rotation of the three apical CO's about a local C_3 axis, as shown for **3** (*Scheme 2*). As the bridging CO's *a* and *b'* do not exchange, the remaining connectivities must be due to a

unique change of basal face by synchronous bridging of three CO's to the (Rh(1)–Ir(1)–Rh(2)) face (*Scheme 3*). The two processes occur at about the same rate in **5**, but are clearly separated in **4**. An EXSY spectrum of **4** in CD_2Cl_2 at 220 K only shows the connectivity $g \leftrightarrow g' \leftrightarrow e$ (*Fig. 4, b*). Simulation of the variable-temperature ^{13}C-NMR spectra of **4** ($190 < T < 250$ K) using the corresponding three site exchange matrix gave a

Scheme 3

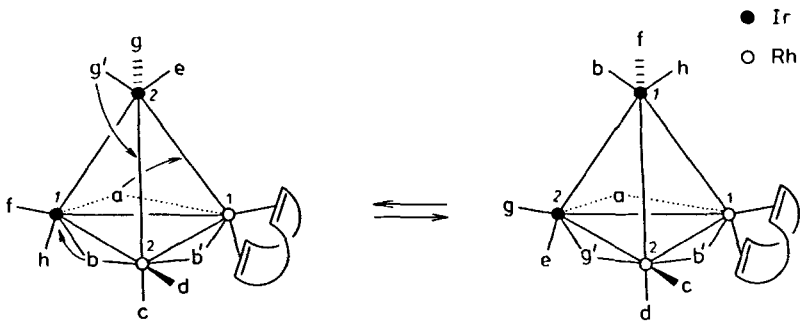

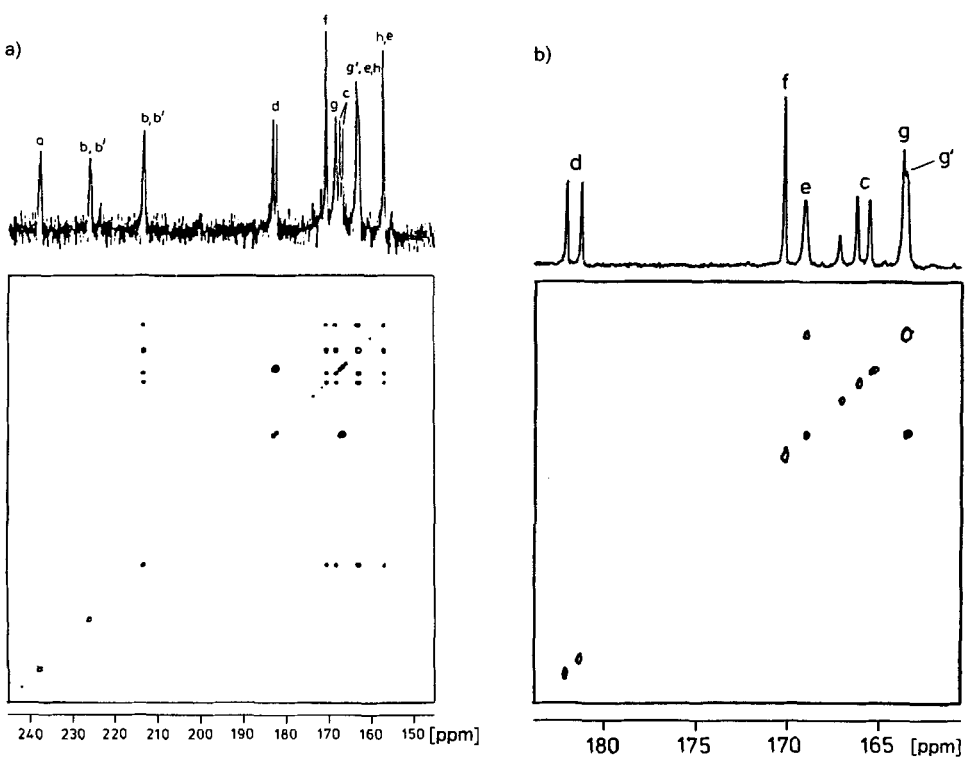

Fig. 4. a) *EXSY Spectrum of* **5** *in* CD_2Cl_2 *at 268 K* (mixing time: 100 ms, $F2 = 9091$, $F1 = 4545.5$ Hz); b) *EXSY spectrum of* **4** in CD_2Cl_2 at 220 K (mixing time: 100 ms, region of terminal CO's, $F2 = 2136$, $F1 = 1068$ Hz)

free enthalpy of activation of 46.6 ± 0.6 kJ mol^{-1} at 298 K for the rotation of the three apical CO's. Above 250 K, apical-basal exchanges are observed, and the same change of basal face as described for **5** starts to contribute significantly to the scrambling of CO's. The change of basal face shown in *Scheme 3* should interchange the radial and axial C=C bonds of the diolefin. Indeed, the ^{1}H-NMR spectrum of **4** is blocked at 228 K (*Experimental*), and upon heating the two resonances due to the pairs of olefinic protons located in radial and axial positions, respectively, coalesce at *ca.* 298 K. The rate constant (k = 552 ± 42 s^{-1}) agrees within experimental error with that of the CO scrambling due to the change of basal face. Simulation of the variable-temperature ^{1}H-NMR spectra using the corresponding two site exchange matrix gave a free enthalpy of activation of 57.1 ± 0.5 kJ mol^{-1} at 298 K for the change of basal face.

The reaction of **1** with excess norbornadiene gave $[Ir_2Rh_2(CO)_8(\eta^4\text{-(nbd)}_2]$ (**6**). The red crystals of **6** are thermally more stable than those of **1**–**5** and were submitted to X-ray analysis (see below) to establish a set of structural data for the new compounds described in the text.

The reaction of **1** with 1 mol-equiv. of tridentate ligands with P- or S-donor atoms gave $[Ir_2Rh_2(CO)_9(\mu_3\text{-L})]$ (L = $HC(PPh_2)_3$ tripod), **7**; L = 1,3,5-trithiane, **8**) in good yields. Both clusters are stable in solution under N_2, but **8** reverts back to **1** under CO (1 atm). Their IR spectra show absorptions below 1900 cm^{-1} indicating the presence of bridging CO's. The ^{31}P-NMR spectrum of **7** in CD_2Cl_2 at 298 K consists of a *doublet* of *quintets* and a *triplet* with relative intensities 2:1 which could be simulated as an *AA'A''XX'* spin system, and with $\Delta\delta$'s ($= \delta_{coord} - \delta_{free\ L}$) typical of axially located P-atoms [9], as in $[Ir_4(CO)_9(tripod)]$ [18]. This spectrum and the ^{1}H-NMR spectrum of **8** are temperature-independent, showing that the ligands L do not participate in the fluxional processes. The ^{13}C-NMR spectra of samples of **7** and **8** enriched in ^{13}CO (*ca.* 30%) in CD_2Cl_2 are blocked at 180 K with six CO resonances indicating C_s symmetry (*Experimental*). Both spectra show a *triplet* (^1J(C,Rh) ≈ 30 Hz) and a *doublet* (^1J(C,Rh) ≈ 26 Hz) with δ's in the region of bridging CO's, and a *doublet* (^1J(C,Rh) ≈ 76 Hz) and *singlet* with δ's in the region of

Scheme 4

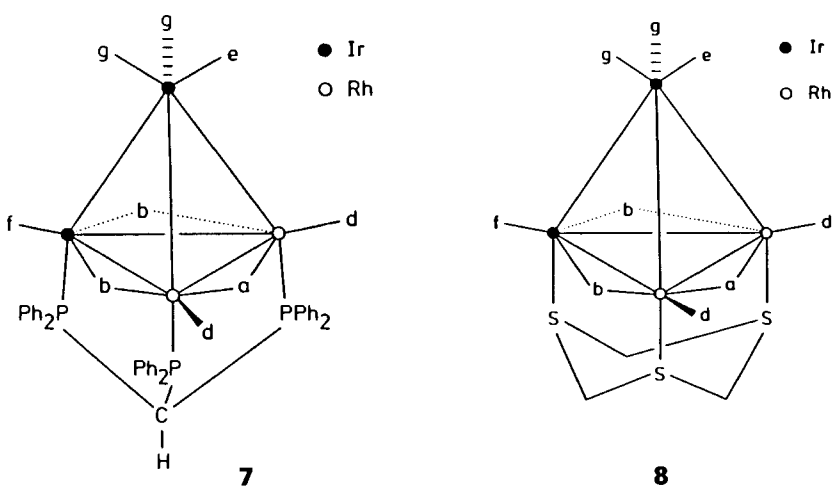

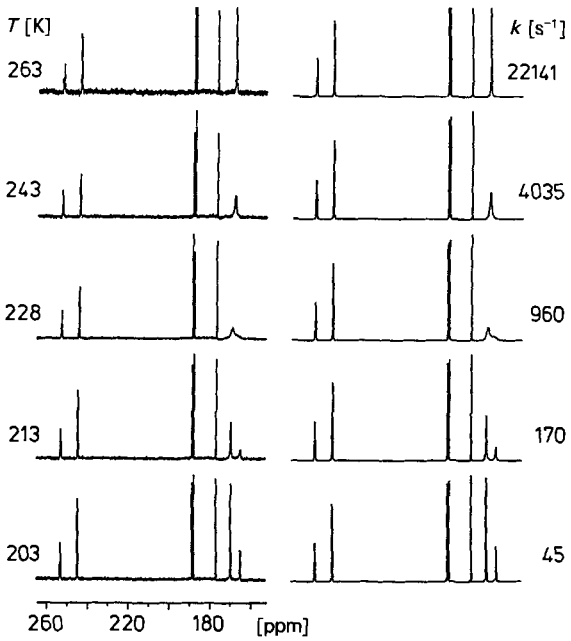

Fig. 5. *Experimental and calculated variable-temperature ^{13}C-NMR spectra of* **8** *in CD_2Cl_2*

radial CO's. Clusters **7** and **8** have thus a triangular $IrRh_2$ unit with three edge-bridging CO's defining a basal face capped by the tridentate ligand (*Scheme 4*). The variable-temperature ^{13}C-NMR spectra of **7** and **8** (*Fig. 5*) show that CO scrambling is restricted to the rotation of three CO's about a local C_3 axis on the axial Ir-atom. Simulation with the corresponding two sites exchange matrix gave free enthalpies of activation of 41.0 ± 0.6 for **7** and 42.0 ± 0.5 kJ mol^{-1} for **8** at 298 K. No exchange of basal CO's was observed close to the boiling point of the solvent in a sealed tube. In contrast, the fluxional process of lowest activation energy in $[Ir_4(CO)_9(1,3,5\text{-trithiane})]$ is the merry-go-round of the six basal CO's with the unbridged isomer as an intermediate, and a $\Delta G^{\neq}$ of 38.0 ± 0.5 kJ mol^{-1} at 298 K [13]. Therefore, substitution of Ir by Rh increases the activation energy of a merry-go-round requiring debridging of a Rh–Rh bond by more than 30 kJ mol^{-1} with respect to the isostructural Ir_4 compound.

In summary, this study shows that, in mixed Ir,Rh carbonyl clusters, the site of intermolecular ligand exchange is the Rh-atom, and that the site of intramolecular CO exchange is preferentially the Ir-atom. The process requiring CO debridging of a Rh–Rh bond are effectively slowed with respect to the corresponding Ir_4 cluster compounds. The clusters $[Ir_2Rh_2(CO)_{11}(PPh_3)]$ and $(Ir_3Rh(CO)_{11}(PPh_3)]$ display a new type of fluxional process where the P-donor ligand is mobile which will be described elsewhere.

Crystal Structure of $[Ir_2Rh_2(CO)_8(\eta^4\text{-NBD})_2]$ (6). – The molecular C_s geometry of **6** is shown in *Fig. 6*. Relevant bond distances and angles are listed in the *Table*. The overall ligand distribution is that common to the majority of substituted Ir_4 and Rh_4 clusters with three edge-bridging CO's defining the basal face of the metal tetrahedron and with the

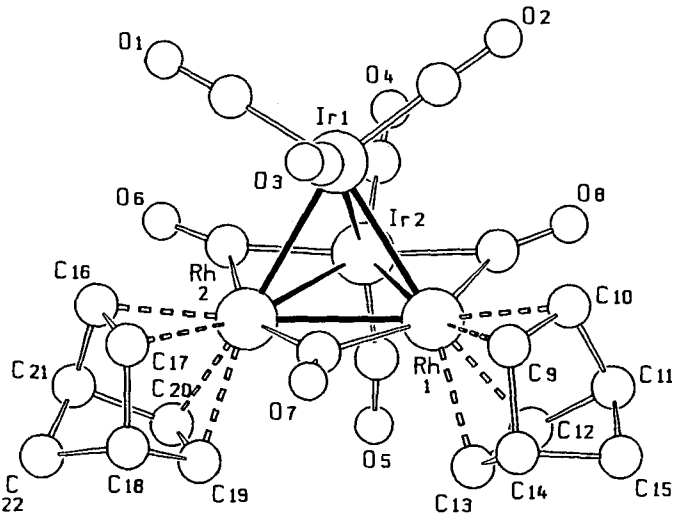

Fig. 6. *Perspective view of* $[Ir_2Rh_2(CO)_5(\mu_2\text{-}CO)_3(\eta^4\text{-}nbd)_2]$ (arbitrary numbering)

Table. *Selected Bond Distances* [Å] *and Angles* [°] *in* $[Ir_2Rh_2(CO)_8(\eta^4\text{-}nbd)_2]$ (**6**). Standard deviations are given in parentheses.

Ir(1)–Ir(2)	2.722(1)	Rh(1)–C(9)	2.18(2)	C(9)–C(10)	1.42(4)
Ir(1)–Rh(1)	2.713(2)	Rh(1)–C(10)	2.21(3)	C(9)–C(14)	1.58(5)
Ir(1)–Rh(2)	2.697(2)	Rh(1)–C(12)	2.25(3)	C(11)–C(12)	1.60(4)
Ir(2)–Rh(1)	2.704(2)	Rh(1)–C(13)	2.29(2)	C(11)–C(15)	1.47(4)
Ir(2)–Rh(2)	2.704(2)	Rh(2)–C(16)	2.24(2)	C(12)–C(13)	1.43(3)
Rh(1)–Rh(2)	2.750(2)	Rh(2)–C(17)	2.23(2)	C(13)–C(14)	1.43(4)
Ir(1)–C(1)	1.90(3)	Rh(2)–C(19)	2.21(3)	C(10)–C(11)	1.49(4)
Ir(1)–C(2)	1.88(4)	Rh(2)–C(20)	2.18(2)	C(14)–C(15)	1.55(4)
Ir(1)–C(3)	1.88(2)	C(1)–O(1)	1.16(4)	C(16)–C(17)	1.36(3)
Ir(2)–C(4)	1.88(3)	C(2)–O(2)	1.17(4)	C(16)–C(21)	1.50(4)
Ir(2)–C(5)	1.91(3)	C(3)–O(3)	1.15(3)	C(17)–C(18)	1.52(4)
Ir(2)–C(6)	1.99(3)	C(4)–O(4)	1.12(3)	C(18)–C(19)	1.55(4)
Rh(2)–C(6)	2.16(3)	C(5)–O(5)	1.13(3)	C(18)–C(22)	1.56(3)
Rh(1)–C(7)	2.11(2)	C(6)–O(6)	1.18(3)	C(19)–C(20)	1.32(4)
Rh(2)–C(7)	2.02(2)	C(7)–O(7)	1.16(3)	C(20)–C(21)	1.60(4)
Ir(2)–C(8)	2.08(2)	C(8)–O(8)	1.15(3)	C(21)–C(22)	1.49(4)
Rh(1)–C(8)	2.14(3)				

O(1)–C(1)–Ir(1)	176(3)	O(7)–C(7)–Rh(2)	141(2)
O(2)–C(2)–Ir(1)	173(3)	O(8)–C(8)–Ir(2)	143(2)
O(3)–C(3)–Ir(1)	174(3)	O(8)–C(8)–Rh(1)	137(2)
O(4)–C(4)–Ir(2)	177(2)	C(1)–Ir(1)–C(2)	108(2)
O(5)–C(5)–Ir(2)	170(3)	C(1)–Ir(1)–C(3)	101(1)
O(6)–C(6)–Ir(2)	147(2)	C(2)–Ir(1)–C(3)	101(1)
O(6)–C(6)–Rh(2)	131(2)	C(4)–Ir(2)–C(5)	100(1)
O(7)–C(7)–Rh(1)	136(2)		

two diolefin ligands replacing both axial and radial terminal CO groups on two Rh-atoms of the basal Rh(1)–Rh(2)–Ir(2) face. The Ir–Rh bonds are slightly shorter than the Ir–Ir bond, the longest bond being that between the two diolefin-coordinated metals. No appreciable shortening of the CO-bridged intermetallic distances with respect to the unbridged ones can be detected as in most Ir_4 and Rh_4 substituted derivatives [19]. The metal–C(diolefin) interactions range from 2.18(2) to 2.29(2) Å without any clear distinction between radial and axial bonds. The C=C bonds average 1.38(4) Å. The values compare well with those previously reported for $[Ir_4(CO)_9L(\eta^4\text{-nbd})]$ (C=C 1.43(3) and 1.32(3); Ir–C 2.20(2) and 2.18(2) Å for L = PMe_2Ph and PPh_3, respectively [20]).

We thank the *Swiss National Science Foundation*, the *Ministero delle Università e della Ricerca Scientifica e Tecnologica*, and the *Fonds Herbette* for the financial support. We thank Prof. *Aime* for the solid-state spectrum of **1**.

Experimental Part

1. *General.* See [21].

2. *Dodecacarbonyldiiridiumdirhodium* (**1**, $[Rh(CO)_2Cl]_2$; 156 mg, 0.4 mmol) and $AgPF_6$ (204 mg, 0.8 mmol) were stirred at 0° in anh. THF (20 ml) for 40 min under Ar. After filtration, the pale-yellow soln. was added dropwise at –50° to a soln. of $PPN[Ir(CO)_4]$ [7] (674 mg, 0.8 mmol) in THF (60 ml)/pentane (20 ml). The soln. was stirred for 60 min, then pentane (50 ml) was added at r.t. Filtration through silica gel and evaporation left an orange residue. Recrystallisation from CH_2Cl_2/hexane at –25° gave **1** (227 mg, 61%) as orange, twinned crystals. IR (CH_2Cl_2): 2072*vs*, 2035*s*, 1926*w*, 1884*s*, 1861*s*. IR (nujol): 2076*vs*, 2018*vs*, 1920*w*, 1880*s*, 1857*s* (CO). ^{13}C-NMR (90.55 Hz): see text. EI-MS (70 eV): 927 (10, M^+), 899 (13), 871 (13), 815 (14, $[M - 4\,CO]^+$), 787 (48), 759 (41), 731 (31), 703 (29), 675 (37), 647 (21), 619 (20), 591 (23, $[M - 12\,CO]^+$), 486 (13, Ir_2Rh), 398 (11, $IrRh_2$), 295 (13, IrRh), 131 (31, RhCO), 103 (100, Rh). The envelope of the molecular peak was in agreement with the relative populations of the isotopomers of Ir_2Rh_2. Anal. calc. for $C_{12}O_{12}Ir_2Rh_2$ (926.4): C 15.56; found: C 15.74. Electron microprobe analysis: Ir/Rh calc. 1.87; found 1.87 ± 0.06.

3. *Substituted Derivatives of* **1**. *Tetraethylammonium Bromoundecacarbonyldiiridiumdirhodate(1–)* (**2**) *and Tetraethylammonium Undecacarbonyliododiiridiumdirhodate(1–)* (**3**). A soln. of **1** (100 mg, 0.108 mmol) and NEt_4Br (115 mg, 0.524 mmol) or NEt_4I (112 mg, 0.435 mmol) in CH_2Cl_2 (50 ml) was stirred under Ar at 0° for 60 min, then at r.t. for 30 min. After evaporation, the residue was extracted into acetone (20 ml) and filtered to eliminate the excess of NEt_4X. The filtrate was evaporated to dryness, and the residue was recrystallised from CH_2Cl_2/Et_2O at –25° giving red microcrystals of **2** (88 mg, 73%) and **3** (93 mg, 76%).

Data of **2**: IR (CH_2Cl_2): 2083*m*, 2053*s*, 2013*s*, 1902*w*, 1850*m*, 1834*m* (CO). ^{13}C-NMR (CD_2Cl_2, 190 K): 236.6 (*dd*, *J*(C,Rh) = 22, 20 Hz, *a*); 228.0 (*d*, *J*(C,Rh) = 34, *b'*); 218.5 (*d*, *J*(C,Rh) = 27, *b*); 184.6 (*d*, *J*(C,Rh) = 80, *d'*); 184.1 (*d*, *J*(C,Rh) = 73, *d*); 172.1 (*s*, *f*); 168.3 (*s*, *g*); 167.7 (*d*, *J*(C,Rh) = 62, *c*); 166.7 (*s*, *g'*); 162.0, 157.6 (2*s*, *e*, *h*). Anal. calc. for $BrC_{19}H_{20}NO_{11}Ir_2Rh_2$ (1108.5): C 20.59, H 1.82, N 1.26; found: C 20.53, H 1.85, N 1.22.

Data of **3**: IR (CH_2Cl_2): 2082*m*, 2051*s*, 2012*s*, 1900*w*, 1847*m*, 1829*m* (CO). ^{13}C-NMR (CD_2Cl_2, 190 K): 233.7 (*dd*, *J* = 22, 20, *a*); 225.2 (*d*, *J* = 33, *b'*); 217.7 (*d*, *J* = 27, *b*); 185.7 (*d*, *J* = 79, *d'*); 183.4 (*d*, *J* = 73, *d*); 171.9 (*s*, *f*); 168.9 (*s*, *g*); 167.2 (*s*, *g'*); 167.0 (*d*, *J* = 64, *c*); 162.7, 157.3 (2*s*, *e*, *h*). Anal. calc. for $C_{19}H_{20}INO_{11}Ir_2Rh_2$ (1155.5): C 19.75, H 1.74, N 1.21; found: C 19.25, H 1.69, N 1.24.

$[Ir_2Rh_2(CO)_{11}Cl]^-$ was only observed in solution, as it decomposed during attempted crystallisation at 0 or –25°. ^{13}C-NMR (CD_2Cl_2, 190 K); 238.5 (*dd*, *J* = 23, 21); 229.7 (*d*, *J* = 34); 219.0 (*d*, *J* = 27); 184.7 (*d*, *J* = 83); 184.6 (*d*, *J* = 67); 172.4, 168.2 (2*s*); 168.1 (*d*, *J* = 62); 166.1, 161.8 (2*s*); all resonances have the same relatives intensities.

Decacarbonyl(2–3-η:5–6-η-norbornadiene)diiridiumdirhodium (**4**) *and Decacarbonyl(1–2-η:5–6-η-cyclooctadiene)diiridiumdirhodium* (**5**). A soln. of **1** (100 mg, 0.11 mmol) and norbornadiene (10 µl, 0.12 mmol) or cycloocta-1,5-diene (13 µl, 0.12 mmol) in CH_2Cl_2 (40 ml) was stirred at 35° for 2 h, following the substitution using TLC. The red suspension was reduced to 10 ml at r.t. and filtered through silica gel. After evaporation, the residue was extracted into CH_2Cl_2 and purified by column chromatography (*Lobar B, Lichroprep Si 60*, 40–63 µm, CH_2Cl_2/hexane 1:2). The first fraction contained unreacted **1** (4%). The second fraction gave **4** (59 mg, 55%) and **5** (63 mg, 60%), as red microcrystals after recrystallisation from CH_2Cl_2/hexane at –25°. A third fraction contained $[Ir_2Rh_2(CO)_8(nbd)_2]$ (4%) and an unidentified cod-containing cluster.

Data of **4**: IR (CH_2Cl_2): 2073*s*, 2051v*s*, 2014*s*, 1882*w*, 1853*m*, 1829*m* (CO). ^{1}H-NMR (CD_2Cl_2, 228 K): 4.97, 4.49 (2*s*, H–C(2,3,5,6)); 4.12, 4.08 (2*s*, H–C(1,4)); 1.35 (*m*, H–C(7a,7s)). At *ca.* 298 K, the resonances of H–C(2,3,5,6) and of H–C(1,4) coalesce into 2 br. *s*, at 4.73 and 4.10 ppm, respectively. ^{13}C-NMR (CD_2Cl_2, 190 K): 236.6 (*td*, J(C,Rh) = 28, J(C,C) = 9, *a*); 223.9, 215.4 (2*dd*, J(C,Rh) = 26, J(C,C) = 8, *b'*, *b*); 181.9 (*d*, J(C,Rh) = 75, *d*); 170.9 (*s*, *f*); 168.9 (*s*, *g*); 165.8 (*d*, J(C,Rh) = 62, *c*); 163.6 (*s*, *g'*); 163.4, 155.5 (2*s*, *h*, *e*). Anal. calc. for $C_{17}H_8O_{10}Ir_2Rh_2$ (962.5): C 21.21, H 0.84; found: C 20.95, H 0.80.

Data of **5** (IR (CH_2Cl_2): 2070*s*, 2051v*s*, 2013*s*, 1881*w*, 1855*m*, 1829*m* (CO). ^{1}H-NMR (CD_2Cl_2, 300 K); 4.75, 3.82, 3.05, 2.75, 2.30, 1.97 (6*m*). ^{13}C-NMR (CD_2Cl_2, 213 K): 238.6 (*td*, J(C,Rh) = 29, J(C,C) = 9, *a*); 226.9, 214.7 (2*dd*, J(C,Rh) = 28, 26, J(C,C) = 8, *b'*, *b*); 183.2 (*d*, J(C,Rh) = 77, *d*); 171.0 (*s*, *f*); 168.7 (*s*, *g*); 167.3 (*d*, J(C,Rh) = 62, *c*); 163.7 (*s*, *g'*); 163.1, 157.2 (2*s*, *h*, *e*). Anal. calc. for $C_{18}H_{12}O_{12}Ir_2Rh_2$ (978.5): C 22.09, H 1.24, Ir + Rh 60.32; found: C 21.84, H 1.09, Ir + Rh 60.05.

Octacarbonylbis(2–3-η:5–6-η-norbornadiene)diiridiumdirhodium (**6**). A soln. of $[Rh_2Cl_2(nbd)_2]$ (461 mg, 0.5 mmol) and $AgPF_6$ (252 mg, 1 mmol) in THF (25 ml) was stirred at 0° for 1 h, then filtered and added dropwise to a soln. of PPN[Ir(CO)$_4$] (843 mg, 1 mmol) in THF (50 ml)/pentane (15 ml) at −50°. The mixture was vigorously stirred for 30 min and filtered through silica gel. Following solvent removal *i.v.*, the residue was extracted into CH_2Cl_2 and purified by column chromatography (*Lobar B*, *Lichroprep Si 60*, 40–63 μm, CH_2Cl_2/hexane 1:3). Recrystallisation from CH_2Cl_2/hexane at −25° gave **6** (220 mg, 45%) as red microcrystals. Anal. calc. for $C_{22}H_{16}O_8Ir_2Rh_2$ (999.6): C 26.46, H 1.61; found: C 26.20, H 1.58.

Nonacarbonyl[μ$_3$-tris(diphenylphosphino)methane]diiridiumdirhodium (**7**). A soln. of $HC(PPh_2)_3$ (92 mg, 0.16 mmol) in toluene (20 ml) was added dropwise to a soln. of **1** (140 mg, 0.15 mmol) in hexane (40 ml), and stirred at 40° for 6 h. The red precipitate was filtered, washed with toluene (5 ml), and dried *i.v.* Recrystallisation from CH_2Cl_2/hexane at −25° gave **7** (145 mg, 68%) as red microcrystals. IR (CH_2Cl_2): 2070*s*, 2010*s*, 1980 (sh), 1850*w*, 1812*m*, 1790*m* (CO). ^{31}P-NMR (CD_2Cl_2, 298 K, H_3PO_4 80% as external reference): −13.1 (*d*, *quint.*, 2 P), −26.8 ppm (*t*, ^1J(P,Rh) = 126.5, ^2J(P,Rh) = 0.2, ^2J(P,P) = 31.4, 1 P). ^{13}C-NMR (CD_2Cl_2, 180 K): 241.6 (*t*, J(C,Rh) = 29.1, *a*); 232.5 (*d*, J(C,Rh) = 25.5, *b*); 193.5 (*d*, J(C,Rh) = 75.9, *d*); 180.0 (*s*, *f*); 170.4 (*d*, ^3J(C,P) = 45.8, *g*); 165.5 (*d*, ^3J(C,P) = 33.9, *e*); the resonances have the relative intensities 1:2:2:1:2:1 in order of decreasing δ's. Anal. calc. for $C_{46}H_{31}O_9P_3Ir_2Rh_2$ (1410.8): C 39.10, H 2.21, P 6.58; found: C 39.55, H 2.42, P 6.34.

Nonacarbonyl(μ$_3$-1,3,5-trithiane)diiridiumdirhodium (**8**). A soln. of **1** (100 mg, 0.108 mmol) and 1,3,5-trithiane (15 mg, 0.11 mmol) in THF (60 ml) was stirred at 0° for 1 h, then refluxed for 1 h under N_2 to achieve the third CO substitution at one Ir-atom, as followed using TLC. After evaporation to dryness, the residue was taken up in CH_2Cl_2 and chromatographed on a thick plate of silica gel (1 mm) using CH_2Cl_2. Crystallisation from CH_2Cl_2/hexane at −25° gave **8** (98 mg, 93%). IR (THF): 2074*m*, 2014*s*, 1979*m*, 1864*w*, 1820*m*, 1796*m* (CO). ^{13}C-NMR (CD_2Cl_2, 183 K): 253.7 (*t*, J(C,Rh) = 30.8, *a*); 245.2 (*d*, J(C,Rh) = 26.4, *b*); 188.4 (*d*, J(C,Rh) = 77.0, *d*); 177.1 (*s*, *f*); 169.7 (*s*, *g*); 164.9 (*s*, *e*); the resonances have the relative intensities 1:2:2:1:2:1 in order of decreasing δ's. Anal. calc. for $C_{12}H_6O_9S_3Ir_2Rh_2$ (980.62): C 14.69, H 0.61, S 9.80; found: C 14.65, H 0.58, S 9.85.

X-Ray Diffraction Measurements of **6**. *Crystal data*: 0.10 × 0.12 × 0.15 mm; orthorhombic; $P2_12_12_1$; a = 11.11(1), b = 12.189(3), c = 17.196(2) Å; V = 2328.7 Å^3; Z = 4; F(000) = 1824. *Data collection*: λ (MoK_α) = 0.71069 Å; μ = 122.9 cm^{-1}; θ range: 2.5–25°; ω-scan width: 0.9°; requested counting σ (I)/I: 0.01; prescan rate: 5 deg min^{-1}; prescan acceptance σ (I)/I: 0.5; maximum scan time: 100 s; octants explored: +h, +k, +l; 2155 measured reflections; 1978 unique observed reflections used in the refinement [$I_0 > 2\sigma(I_0)$]; min. and max. absorption corrections: 0.68 and 1.00, respectively; R = 4.6%; R_w = 5.0%. The structure was solved using direct methods and subsequent difference *Fourier* syntheses. The structural model was refined by least-squares calculations. For all calculations, the SHELX package of crystallographic programs was used [22]. Absorption corrections were applied by the *Walker* and *Stuart* method [23], once the complete structural model was obtained and all atoms refined isotropically. All non-H-atoms were refined anisotropically, while single isotropic temp. factors were refined for the H-atoms [0.06(2) Å^2]. H-Atoms were added in calculated positions (C–H = 1.08 Å) and not refined, although their contribution to the structure factors was taken into account. Residual electron density peaks (*ca.* 2 e/Å^3) were found in the proximity of the metal atoms. Lists of observed and calculated structure factors, of crystal data, of fractional atomic coordinates and anisotropic thermal parameters, and of interatomic distances and angles are deposited at *Cambridge Structural Database*.

REFERENCES

[1] S. Martinengo, P. Chini, V.G. Albano, F. Cariati, T. Salvatori, *J. Organomet. Chem.* **1973,** *59,* 379.
[2] V.G. Albano, G. Ciani, S. Martinengo, *J. Organomet. Chem.* **1974,** *78,* 265.
[3] B.F.G. Johnson, J. Lewis, T.W. Matheson, *J. Chem. Soc., Chem. Commun.* **1974,** 441.
[4] T.A. Pakkanen, J. Pursiainen, T. Venäläinen, T.T. Pakkanen, *J. Organomet. Chem.* **1989,** *372,* 129.
[5] G. Bondietti, Thèse de doctorat n° 1135, EPFL-Lausanne, 1993.
[6] J.E. Ellis, P.T. Barger, M.L. Winzenburg, *J. Chem. Soc., Chem. Commun.* **1977,** 686.
[7] L. Garlaschelli, P. Chini, S. Martinengo, *Gazz. Chim. Ital.* **1982,** *112,* 285; L. Garlaschelli, R. Della Pergola, S. Martinengo, *Inorg. Synth.* **1991,** *28,* 211.
[8] R.R. Schrock, J.A. Osborn, *J. Am. Chem. Soc.* **1971,** *93,* 3089.
[9] R. Ros, A. Scrivanti, V.G. Albano, D. Braga, L. Garlaschelli, *J. Chem. Soc., Dalton Trans.* **1986,** 2411.
[10] G.F. Stuntz, J.R. Shapley, *J. Organomet. Chem.* **1981,** *213,* 329.
[11] F.A. Cotton, L. Kruczynski, B.L. Shapiro, L.T. Johnson, *J. Am. Chem. Soc.* **1972,** *94,* 6191; J. Evans, B.F.G. Johnson, J. Lewis, J.R. Norton, F.A. Cotton, *J. Chem. Soc., Chem. Commun.* **1973,** 807.
[12] K. Besançon, Thèse de doctorat, Université de Lausanne, 1993.
[13] A. Orlandi, U. Frey, G. Suardi, A.E. Merbach, R. Roulet, *Inorg. Chem.* **1992,** *31,* 1304.
[14] EXCHANGE, program library, Computing Center, University of Lausanne.
[15] A. Strawczynski, R. Ros, R. Roulet, *Helv. Chim. Acta* **1988,** *71,* 867; A. Strawczynski, G. Suardi, R. Ros, R. Roulet, *Helv. Chim. Acta,* submitted.
[16] G.F. Stuntz, J.R. Shapley, C.G. Pierpont, *Inorg. Chem.* **1978,** *17,* 2596.
[17] R. Ros, A. Scrivanti, R. Roulet, *J. Organomet. Chem.* **1988,** *303,* 273; A. Strawczynski, R. Ros, R. Roulet, F. Grepioni, D. Braga, *Helv. Chim. Acta* **1988,** *71,* 1885.
[18] J.A. Clucas, M.M. Harding, B.S. Nicholls, K. Smith, *J. Chem. Soc., Chem. Commun.* **1984,** 319.
[19] D. Braga, F. Grepioni, *J. Organomet. Chem.* **1987,** *336,* C9.
[20] D. Braga, F. Grepioni, G. Guadalupi, A. Scrivanti, R. Ros, R. Roulet, *Organometallics* **1987,** *6,* 56.
[21] A. Orlandi, R. Ros, R. Roulet, *Helv. Chim. Acta* **1991,** *74,* 1464.
[22] G.M. Sheldrick, SHELX76, Program for Crystal Structure Determination, Cambridge, U.K., 1976.
[23] N. Walker, D. Stuart, *Acta Cryst., Sect. A* **1983,** *39,* 158.